Tertiary Current Distributions on the Wafer in a Plating Cell

Lizhu Tong[1]
[1]Kesoku Engineering System Co., Ltd.
1-9-5 Uchikanda, Chiyoda-ku, Tokyo 101-0047, Japan, tong@kesco.co.jp

Abstract: The tertiary current distributions on the wafer in a plating cell are studied in this work. An acid copper sulfate electrolyte composed of $CuSO_4 \cdot 5H_2O$ of 2.4 g/L and H_2SO_4 of 90 g/L is taken into account for copper deposition on the wafer. The solution of shear-plate agitating fluid dynamics is coupled into the calculation of tertiary current distributions. The obtained distributions of tertiary current densities and ion concentrations on the wafer present an oscillating wave form, indicating the strong effect of shear-plate agitation on the current distributions. The distance between the wafer and shear plate is analyzed, which determines the oscillating breadth of the tertiary current distributions on the wafer.

Keywords: Electrodeposition, Shear-plate fluid agitation, Tertiary current distribution, COMSOL Multiphysics.

1. Introduction

The reciprocating paddle cell is a known practical method for depositing alloy films on wafer substrates [1~3]. Recently, the mass transfer boundary layer within an industrial wafer plating cell was studied based on the measurement of limiting current [4]. It was indicated that a shear-plate fluid agitation mechanism is capable of generating a thin (*i.e.*,<10 μm), spatially uniform and nonperiodic boundary layer across the entire wafer. Since the current density on the wafer controls the deposited film distribution, the acquirement of the current distributions on the wafer becomes a key to govern the quality of the deposited film on the wafer.

It is known that at currents much below the limiting current, the solution of the current density can be regarded as the potential theory problem [5], *i.e.*, the current distribution is determined by the ohmic potential drop in the solution and the electrode overvoltage, termed as secondary current distribution, in which the current distribution determined only by the ohmic potential drop in the solution is termed as primary current distribution. However, in the cases close to the limiting current, diffusion and convective transport become essential [6], which was termed as the tertiary current problem by Averill and Mahmood [7].

The investigations of the tertiary current distributions in rotating electrodes (RDE) [8] and rotating cylinder Hull (RCH) cells [9] have been reported. However, the tertiary current distribution in an industrial plating cell, especially for the case with a shear-plate fluid agitation, is still not clear. In this work, we coupled the calculations of fluid flows and current distributions in a plating cell. The tertiary current distributions on the wafer were obtained. The effect of the shear-plate fluid agitation on the current distributions on the wafer was presented and discussed.

2. Numerical Model

The model geometry used in this work is shown in Fig. 1. It is known that the Reynolds number for the geometry can be defined by $R_e = UL/\nu$ [4], where U is the line shear plate velocity, L is the shear plate thickness, ν is the kinematic viscosity of the fluid. In the present research the Reynolds number is $R_e \leq$ ~785. The previous research on the reciprocating paddle has

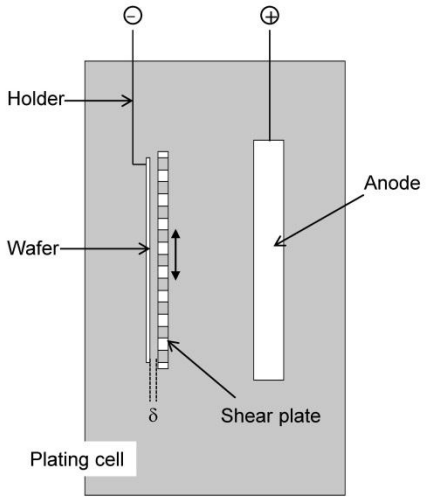

Figure 1. Schematic of the plating cell with shear-plate fluid agitation.

indicated that the wake dynamics of a blunt body in this Reynolds number regime are controlled more by pressure fields than by viscous diffusion and consequently, a laminar model may reasonably predict the dominant flow features for the purpose of estimating the mass-transfer on the wall [1]. Therefore, in this work the laminar flows are taken into account by [10]

Continuity equation

$$\nabla \cdot (\rho \mathbf{u}) = 0, \tag{1}$$

Momentum equation

$$\rho \frac{\partial \mathbf{u}}{\partial t} + \rho \mathbf{u} \cdot \nabla \mathbf{u} = -\nabla p + \nabla \cdot \Big(\mu (\nabla \mathbf{u} + (\nabla \mathbf{u})^T) - \frac{2}{3} \mu (\nabla \cdot \mathbf{u}) \mathbf{I} \Big) + \mathbf{F}, \tag{2}$$

where ρ is the density, $\mathbf{u}$ is the velocity vector, p is the pressure, $\mathbf{F}$ is the volume force vector, $\mathbf{I}$ is the identity matrix.

The material balance equation for the species i in the electrolyte is calculated [10]

$$\frac{\partial c_i}{\partial t} + \nabla \cdot \left(-D_i \nabla c_i - z_i u_{m,i} F c_i \nabla \phi_l + c_i \boldsymbol{u} \right) = R_{i,tot}, \tag{3}$$

where c_i is the concentration of species i, D_i is the diffusion coefficient of species i, z_i is the charge number of species i, $u_{m,i}$ is the mobility of species i, F is Faraday's constant, and ϕ_l is the electrical potential. The current density $\mathbf{i}_l$ in the electrolyte is

$$\mathbf{i}_l = F \sum_{i=1}^{n} z_i \left(-D_i \nabla c_i - z_i u_{m,i} F c_i \nabla \phi_l \right), \tag{4}$$

and then the charge balance in the electrolyte becomes

$$\nabla \cdot \mathbf{i}_l = Q_l, \tag{5}$$

where, Q_l can here be any source or sink. Also, the equation for the electroneutrality condition is considered by

$$\sum z_i c_i = 0. \tag{6}$$

It is known that the local current density on the electrode is related to the local overvoltage, η on the electrode, which is the potential difference between the electrode, V, and the solution adjacent to the electrode, ϕ_0, *i.e.*, $\eta = V - \phi_0$. The overvoltage η can be adequately related to the magnitude of the local current density. In this work, η is approximated by a linear expression from the Butler-Volmer equation at low current density [4]

$$\eta = \frac{i}{i_0} \frac{RT}{(\partial_a + \partial_c) 2F}. \tag{7}$$

The sum of transfer coefficients, $\partial_a + \partial_c$, has a theoretical value of 2. The exchange current density, i_0, can be expressed by [4,6]

$$i_0 = \left(\frac{c_w}{c_b} \right)^{\gamma} i_0(c_b) \tag{8}$$

where c_w is the surface concentration on electrode and c_b is the bulk concentration. γ is the factor representing the effect of concentration on current density.

Equations (1)-(8) are solved using the finite element simulation software COMSOL Multi-physics 4.3. The calculation of fluid flows is coupled into the Electrodeposition module [10].

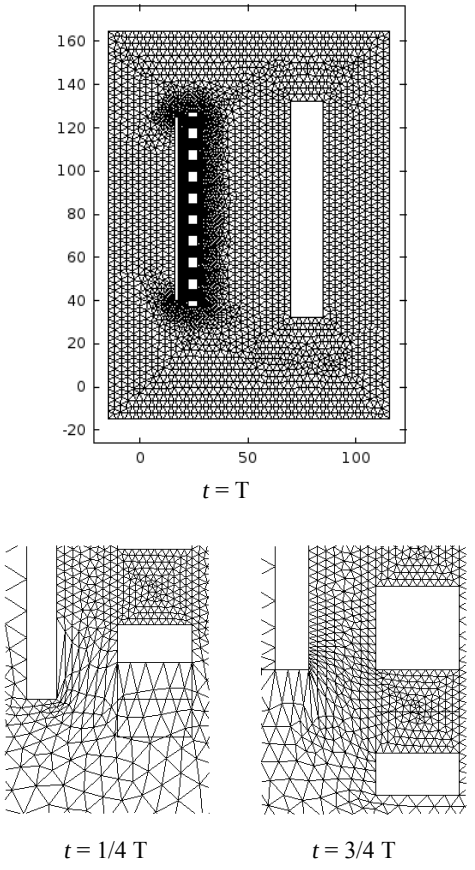

Figure 2. Computational mesh for δ = 4 mm at t = T and locally enlarged meshes at t =1/4 T and 3/4 T. T is the reciprocating period of shear plate.

Table 1: Parameters used in the present research [4,6].

Shear plate
Dimension: 5 mm thickness and 90 mm height
Stroke length, S: 5 mm
Reciprocating frequency: 5 Hz
Distance between wafer and shear plate, δ: 2-6 mm
Electrolyte properties
Density: 1000 kg/m^3
Kinematic viscosity: 1×10^{-6} m^2/s
Bulk concentration of cupric ions: 9.6 mol/m^3
Diffusion coefficient of cupric ions: 5.37×10^{-10} m^2/s
Electrode characteristics
Factor for the effect of concentration, γ: 0.6
Exchange current density, $i_0(c_b)$: 10 A/m^2
Average current density on the wafer: 10 A/m^2

The reciprocation of shear plate is simulated by moving mesh (ale) provided in COMSOL Multiphysics. The computational mesh is presented in Fig.2, in which the locally enlarged meshes at the different phases in a reciprocating cycle are also given. The computational parameters considered are shown in Table 1.

3. Results

The computations are performed for obtaining the distributions of fluid flows and tertiary current densities in a plating cell. The solved domain is limited up to the interface between air and solution. The boundary for the interface is regarded as free-slip wall and the bottom and side boundaries as well as the surfaces of electrodes are stationary no-silp walls. The boundaries for shear plate walls are defined as moving walls with the reciprocating velocity. The obtained results include the distributions of velocity and pressure of fluid flows, ion concentrations, potential, and current densities at the different phases of the reciprocating cycle.

Figure 3 shows the computational results of velocity and pressure of fluid flow, and current density for the distance between wafer and shear plate of δ = 4 mm at t = 1/4 T ($\varphi = \pi/2$). T ($\varphi = 2\pi$) is the reciprocating period of shear plate. The calculations show that the sharp variation of flow velocity appears around the shear plate wall, in which the maximum value arrives at 0.21 m/s. The pressure is changed with the reciprocation of

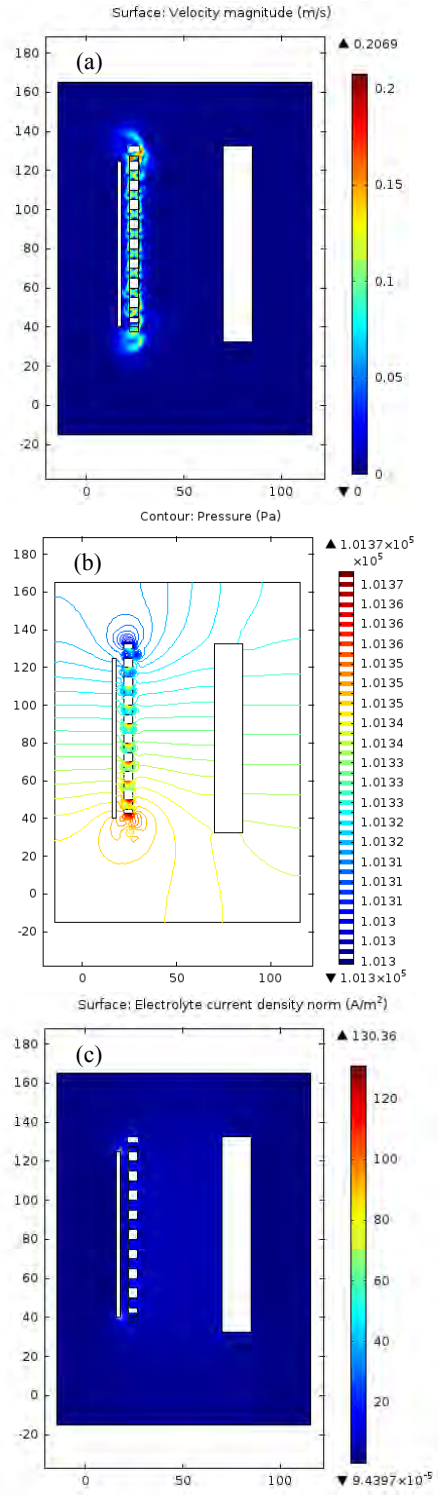

Figure 3. Computational results of (a) velocity, (b) pressure, (c) current density for δ = 4 mm at t = 1/4 T. T is the reciprocating period of shear plate.

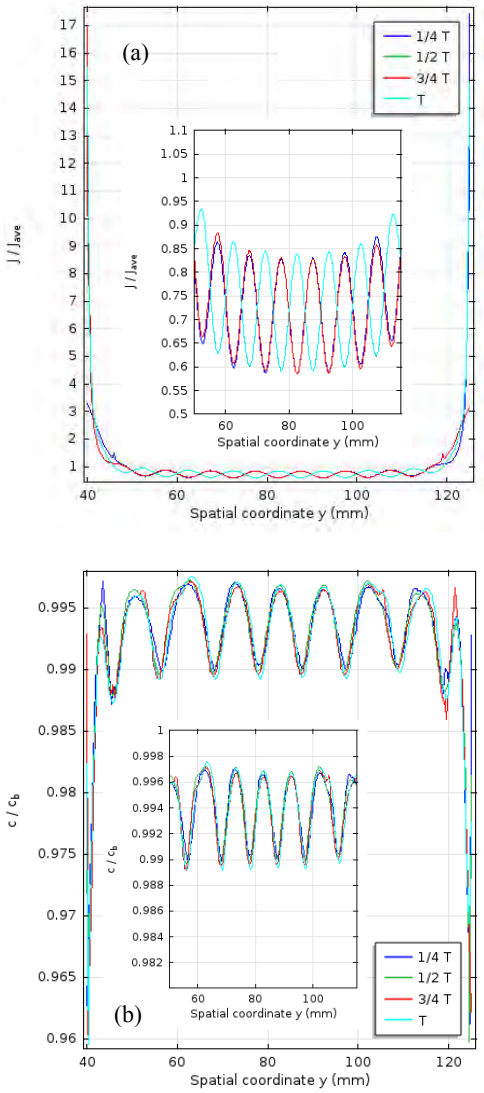

Figure 4. Reduced distributions of (a) current densities and (b) cupric ion (Cu^{2+}) concentrations on the wafer for δ = 4 mm at *t* = 1/4 T. T is the reciprocating period of shear plate.

shear plate. The largest current densities appear at the two terminals of the wafer, which arrive at 130.36 A/m^2, being over ten times more than the average current density (~10 A/m^2) on the wafer. The current distributions on the wafer as shown in Fig. 4(a) also show the properties. The current distributions on the wafer present an oscillating wave form, which can be deduced by a fact that due to the existence of shear plate, the electric field varies with the reciprocation of shear plate. Also, the local current density on the wafer is related to the local overvoltage, as indicated by eqs. (7) and (8). There then exists the influence of cupric ion (Cu^{2+}) concentrations on the current distributions. The distributions of cupric ion (Cu^{2+}) concentrations on the wafer are given in Fig. 4(b).

In this work, the distance between wafer and shear plate, δ, is studied. The computations are performed for δ = 2, 3, 4, 5, 6 mm. Figure 5 shows the tertiary current distributions on the wafer for δ = 2, 3, 4 mm, in which the effects of the terminals of the wafer are omitted. It is obvious that when the distance between the wafer and shear plate increases, the oscillation of tertiary current distributions on the wafer becomes small. The oscillating breadth of current distributions for δ = 4 mm is about three times less than that for δ = 2 mm. The controlling of the distance between the wafer and shear plate could govern the tertiary current distribution on the surface of wafer.

4. Conclusions

This paper presented the study of tertiary current distributions on the wafer in an industrial plating cell. The coupled solution of fluid equations and mass-transport equations were performed. The copper electrodepostion from an acid sulfate electrolyte composed of $CuSO_4 \cdot 5H_2O$ of 2.4 g/L and H_2SO_4 of 90 g/L was considered in this work. The distribution of tertiary current density was calculated on the basis of the simulation of the shear-plate agitated fluid flow.

The simulation results included the velocity and pressure of fluid flows, ion concentrations, potential, and current densities in a plating cell. The calculations were performed for the different distances between the wafer and shear plate. The study of the distance between the wafer and shear plate allows us to control the current distributions on the wafer so as to further improve the quality of the deposited film in the plating cell in future.

5. References

1. G.J. Wilson, P.R. McHugh, "Unsteady numerical simulation of the mass transfer within a reciprocating paddle electroplating cell", *J. Electrochem. Soc.*, **152** (6), C356-C365 (2005)
2. D.T. Schwartz, B.G. Higgins, P. Stroeve, D.

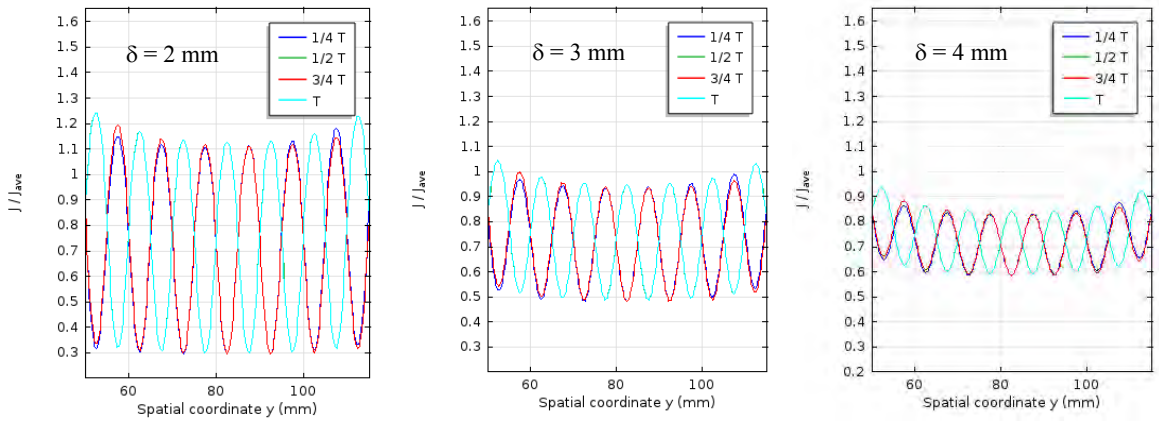

Figure 5. Tertiary current distributions on the wafer for δ = 2 , 3, 4 mm at the different phases of the reciprocating cycle.

Borowski, "Mass-transfer studies in a plating cell with a reciprocating paddle", *J. Electrochem. Soc.*, **134** (7), 1639-1645 (1987)

3. D.E. Rice, D. Sundstrom, M.F. McEachern, L.A. Klumb, J.B. Talbot, "Copper electro-deposition studies with a reciprocating paddle", *J. Electrochem. Soc.*, **135** (11), 2777-2780 (1988)

4. B.Q. Wu, Z. Liu, A. Keigler, J. Harrell, "Diffusion boundary layer studies in an industrial wafer plating cell", *J. Electrochem. Soc.* **152** (5), C272-C276 (2005).

5. L.Z. Tong, K. Ohara, F. Asa, Y. Sugiura, "CFD analysis of eductor agitation in electro-plating tank", *Trans. Inst. Met. Finish.*, **88**(4), 185-190 (2010)

6. J.S. Newman, K.E. Thomas-Alyea, *Electro-chemical systems*, 3rd ed., John Wiley & Sons, Hoboken, NJ (2004)

7. A.F. Averill, H.S. Mahmood, "Determination of tertiary current distribution in electro-deposition cells – Part 1 Computational techniques", *Trans. Inst. Met. Finish.*, **75**(6), 228-233 (1997)

8. L.Z. Tong, "Simulation study of tertiary current distributions on rotating electrodes", *Trans. Inst. Met. Fin.*, **90** (3), 120-124 (2012)

9. C.T.J. Low, E.P.L. Roberts, F.C. Walsh, "Numerical simulation of the current, potential and concentration distributions along the cathode of a rotating cylinder hull cell", *Electrochim. Acta*, **52**, 3831-3840 (2007)

10. COMSOL Multiphysics 4.3- user's guide for CFD Module and Electrodeposition Module and also http://www.comsol.com